Journal of Applied Electrochemistry **32**: 775–781, 2002.
© 2002 *Kluwer Academic Publishers. Printed in the Netherlands.*

Inhibition of corrosion of steel in produced water of Western Desert crude oil

F.M. MAHGOUB[1], B.A. ABD EL-NABEY[2], S.A. EL-KHARASHI[3], M. ATTEYA[3], M.SH. RAMADAN[2] and E. KHAMIS[2,*]
[1]*Department of Material Science, Institute of Graduate Studies and Research, Alexandria University, Egypt*
[2]*Department of Chemistry, Faculty of Science, Alexandria University, Egypt*
[3]*Alexandria Petroleum Company, Alexandria, Egypt*
*(*author for correspondence)*

Received 8 February 2001; accepted in revised form 9 March 2002

Key words: corrosion, crude oil, inhibitors, S-alkyl isothioronium halides, steel

Abstract

The corrosion inhibition of steel in water from Western Desert (Egypt) crude oil by nine S-alkyl isothioronium halides was studied using open-circuit potential (OCP) measurements and potentiodynamic polarization tests . The objectives were to determine (a) the effect of chain length of the alkyl groups on the inhibition efficiency, (b) the effect of halide counter ion on the performance of the inhibitor, and (c) to apply a recent developed kinetic-thermodynamic model on the data and compare it with common adsorption isotherms. The number of active sites, binding constant and change of free energy of adsorption were computed for all inhibitors studied. The inhibition efficiency was correlated with the molecular structure of the inhibitors. It was found that each organic molecule replaces more than one adsorbed water molecule from the steel surface. Potentiodynamic polarization curves indicated that the compounds acted as mixed-type inhibitors. The OCP measurements showed that adsorption of S-alkyl isothioronium compounds at the steel surface is through two adsorbed layers.

1. Introduction

The extent of corrosion problems in the oil and gas industries depends on the fluid composition such as oil type, oil-to-water ratio, water salinity and gas type. The role of water, dissolved oxygen, CO_2, H_2S, dissolved salts, pH, temperature, and velocity on corrosion control of steel in oil fields has been discussed and addressed by several authors [1–6]. The use of corrosion inhibitors in petroleum production is essential for corrosion control in these highly corrosive environments [7–9]. In most cases, corrosion inhibition is found to increase with increase in water salinity and oil-to-water ratio [10]. These findings indicate that the fluid characteristics must be carefully considered in the evaluation and selection of corrosion inhibitors. TAL-25B inhibitor with two benzol rings in its molecule is found to inhibit the corrosion of steel in waste water from oil fields over wide ranges of temperature and flow rate of the corrosive media [11]. Calcium sulfonate, synthetic fatty acid diethanolamide, and oxidized petrolatum are used as corrosion inhibitors for steel in film forming inhibited oil compositions [12]. A corrosion inhibitor containing oleic imidazoline and its precursor oleic amide species is used for the oil–water–iron system [13]. The imidazoline material was preferentially oil soluble and had only sparing solubility in the water phase. It did, however, show a significant tendency to accumulate at the oil/water interface forming a resistive barrier to corrosion. The adsorption of oleic imidazoline from oil onto oil-wet iron was found to hydrophobize the metallic surface and followed a Langmuir isotherm.

In our laboratory, several S-alkyl isothiodoronium halides have been investigated as corrosion inhibitors for acid corrosion of steel. The results indicated that the compounds act as good inhibitors [14]. The present study aimed to throw light on the corrosion of steel in water of Western Desert (Egypt) crude oil in the presence of nine different S-alkyl isothioronium halides as corrosion inhibitors. The work also aims to apply a recent developed kinetic-thermodynamic model and compare the results with those from fitting to common adsorption isotherms.

2. Experimental details

The effect of addition of S-alkyl isothioronium halides on the dissolution rate of steel in water associated with Western Desert crude oil was evaluated at room temperature using open circuit potential (OCP) and potentiodynamic polarization measurements. Commercial steel with chemical composition: C 0.170; S 0.008; Mn 1.180; P 0.008; Si 0.270; Ni 0.040; Cr 0.040 and Mo

Table 1. Chemical analysis of the produced water of Western Desert crude oil, Egypt

Corrosive element	Test method ASTM	ppm
Total dissolved slats (TDS)	D – 1888	76 680.0
Sodium as Na^+	D – 3561	24 050.0
Potassium as K^+	D – 3561	420.0
Calcium as Ca^{2+}	D – 511	1760.0
Magnesium as Mg^{2+}	D – 511	3200.0
Chloride as Cl^-	D – 512	60 350.0
Sulphate as SO_4^{2-}	D – 516	370.0
Bicarbonate as HCO_3^-	D – 1067	568.0
Silicate as SiO_2^-	D – 859	11.4
pH		6.9

0.010 wt % was employed as working electrodes. The potential of a steel electrode was measured relative to a saturated calomel electrode (SCE) from the moment of steel immersion in the electrolyte until steady state was reached. Potentiodynamic polarisation plots for steel were generated using a Wenking potentiostat (model MP 87). The working electrode was a steel rod with cross-section area of 1.2 cm^2. Before measurement, the specimens were ground on a series of emery papers down to 1200 grit. The rods were washed thoroughly with distilled water and dried with ethanol. All experiments were thermostated at 25 ± 0.1 °C. The sweep rate used in this study was 0.5 mV s^{-1}.

The test solution used was water produced from Western Desert (Egypt) crude oil free of oils and greases. A typical chemical composition is given in Table 1. The compounds studied and their symbols are given in Table 2. The general formula of S-alkyl isothioronium halide inhibitors used in this study is

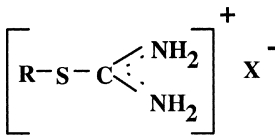

(1)

where R is methyl, ethyl, *n*-propyl, *n*-butyl, *n*-pentyl, *n*-hexyl, *n*-heptyl or *n*-octyl; and X is iodine or bromine. The S-*n*-alkyl isothioronium halides were prepared by mixing equimolecular amounts of thiourea and alkyl halide in acetone, then refluxing for six hours in a water bath [14]. In this process, the following reaction takes place:

Table 2. Investigated compounds

Symbol	Inhibitor
I	S-methyl isothioronium iodide
II	S-ethyl isothioronium iodide
III	S-*n*-propyl isothioronium iodide
IV	S-*n*-butyl isothioronium iodide
V	S-*n*-pentyl isothioronium iodide
VI	S-*n*-hexyl isothioronium iodide
VII	S-*n*-heptyl isothioronium iodide
VIII	S-*n*-octyl isothioronium iodide
IX	S-*n*-octyl isothioronium bromide

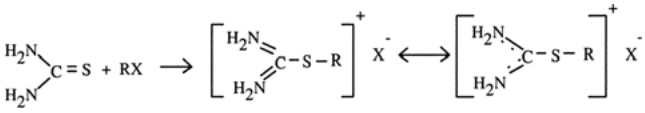

(2)

All additive salts were double crystallized from ethyl alcohol and dried in a vacuum oven. Subsequently powders were prepared using quartz mortars and stored over $CaCl_2$. The inhibitor efficiency was determined using the following relationship:

$$P = \left(1 - \frac{i_{corr}}{(i_{corr})_o}\right) \times 100 \quad (3)$$

where i_{corr} and $(i_{corr})_o$ are the corrosion current densities in the presence and in the absence of inhibitor, respectively.

3. Results and discussion

3.1. *Effect of the number of carbon atoms in S-alkyl isothioronium iodide on corrosion inhibition*

The time dependence of the open circuit potential (OCP) of steel coupons immersed in the produced water was monitored in the absence and presence of various concentrations of S-alkyl isothioronium iodides until steady-state was established. Figure 1 shows the time-dependence of the OCP with or without additions of compound II. Two different trends are observed depending on the inhibitor concentration. For very dilute inhibitor concentrations ($C \leqslant 1 \times 10^{-5}$ M), the OCP decreased (i.e., became more negative) with time until steady state was reached. At higher concentrations of inhibitor ($C > 1 \times 10^{-5}$ M) and at the beginning of OCP, the potential of the test coupons inverts its direction towards less negative values with passage of immersion time.

This behaviour can be explained in terms of adsorption of S-alkyl isothioronium compounds at the steel surface through two adsorbed layers. At low concentrations, the first adsorbed layer is formed. Saturation of this layer is achieved at a certain critical concentration. The values of these critical concentrations for the different inhibitors are given in Table 3. Generally speaking, Table 3 shows that the critical concentration decreases significantly from 10^{-5} M for compound I to 5×10^{-7} M for compounds VI–VIII. This is mostly related to increase in the length of the alkyl chain, that is, to an increased number of carbon atoms in the inhibitor molecule. The outcome indicates that the protection efficiency increases from compound I to compound VIII. Further increasing of the inhibitor concentration leads to the formation of a second adsorbed layer. The effect of the inhibitor concentration on the steady-state potential of steel after 300 min of immersion is shown in Figure 2. The curves have a

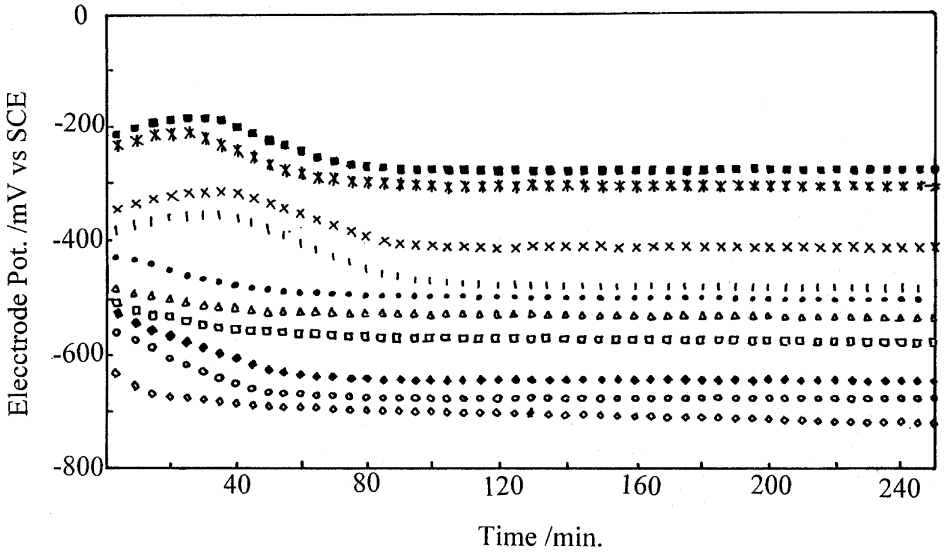

Fig. 1. Change in OCP of steel with time in test solution containing different concentrations of S-ethyl isothioronium iodide. Key: (◇) blank, (○) 1×10^{-7}, (♦) 5×10^{-7} , (□) 1×10^{-6}, (△) 5×10^{-6}, (●) 1×10^{-5}, (+) 5×10^{-5}, (×) 1×10^{-4}, (✳) 1×10^{-3} and (■) 5×10^{-3} M.

Table 3. Relationship between number of carbon atoms in the S-alkyl isothioronium iodide and the critical concentration of each compound

Number of C atoms in inhibitor	Critical concentration/M
1	1×10^{-5}
2	5×10^{-6}
3	1×10^{-6}
4	1×10^{-6}
5	1×10^{-6}
6	5×10^{-7}
7	5×10^{-7}
8	5×10^{-7}

double-S shape. Along the lower S-shape part, at dilute inhibitor solutions, the first adsorbed layer of inhibitor is presumably formed. At the lower part of the upper S curve, saturation of the first adsorbed layer is attained. On increasing the inhibitor concentration, the formation of the second adsorbed layer takes place. Figure 2 also shows that, as the concentration of the inhibitor increases, the OCP at steady-state is shifted towards less negative (i.e., more noble) direction in the following order: VIII > VII > VI > V > IV > III > II > I.

The substitution of the methyl group in the isothioronium iodide compounds by larger alkyl groups with higher nucleophilic power thus leads to a shift of the OCP towards less negative values. This behaviour reflects the increased adsorbability due to the higher electron density on the functional group (which is most probably S–C $(NH_2)_2^+$). This higher electron density leads to easier bond formation, greater adsorption and, consequently, higher inhibition efficiency. In addition, the increase in length of the hydrocarbon chain in the inhibitor molecule, means a more bulky molecule, which screens the surface from attack [15].

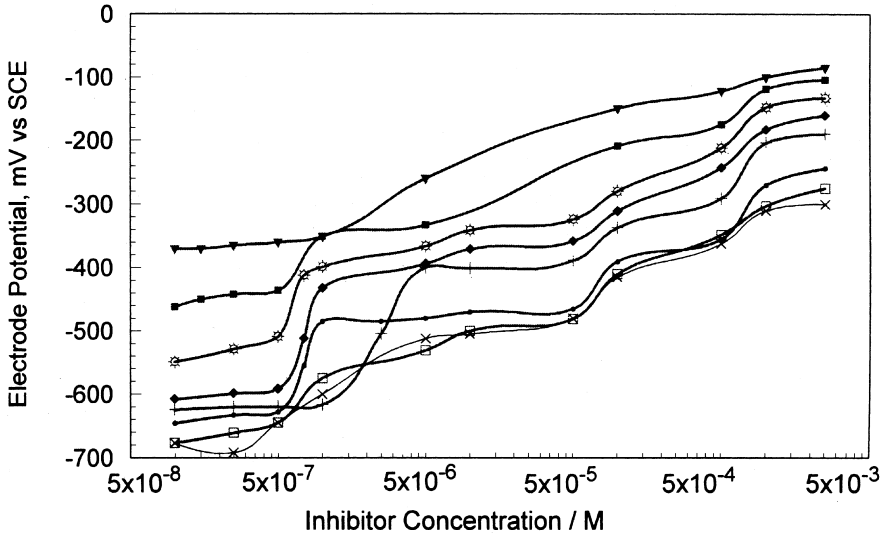

Fig. 2. Change in OCP of steel with concentration of different inhibitors. Key: (×) I, (□) II, (●) III, (+) IV, (♦) V, (✲) VII, (▼) VIII.

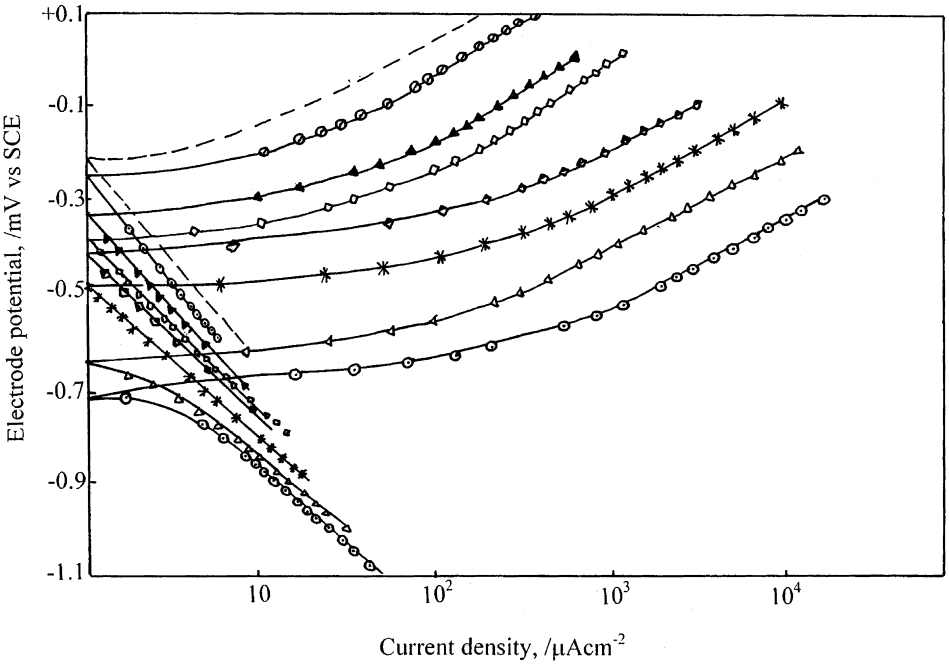

Fig. 3. Polarization curves of steel in test solution containing different concentrations of compound S-*n*-propyl isothioronium iodide. Key: (⊙) 0.0, (△) 5×10^{-7}, (✳) 1×10^{-6}, (◆) 5×10^{-6}, (◇) 1×10^{-5}, (▲) 5×10^{-5}, (ø) 5×10^{-4} and (– – –) 3×10^{-3} M.

Anodic and cathodic polarization curves for steel in test solution with or without additions of S-alkyl isothioronium iodides were obtained at 25 °C. Figure 3 shows the electrochemical polarization behaviour of steel in test solution containing different concentrations of S-*n*-propyl isothioronium iodide (III). It is evident that the presence of the inhibitor retards both the metal dissolution and the cathodic processes acting as a mixed-type inhibitor and the corrosion current density (I_{corr}) decreases with increasing concentration of inhibitor.

A comparison between the inhibitor efficiencies of the S-alkyl isothioronium iodides (I–VIII) at 25 °C is shown in Figure 4. The curves have characteristics of double S-shaped adsorption isotherms, indicative of a two-layer adsorption mechanism for the inhibition process. Along the lower part of the first S curve, corrosion is greatly reduced due to the formation of the first adsorbed layer. Saturation of this layer occurs at a concentration of about 10^{-6} M. Upon further increase of the inhibitor concentration, the efficiency is greatly increased suggesting the formation of the second adsorbed layer. The effect of the inhibitors on the corrosion parameters of the steel in the produced water shows three major characteristics. First, the presence of the inhibitor has little effect on the anodic and cathodic Tafel slopes. This indicates that the adsorption of the S-alkyl isothioronium iodide molecules at the steel surface retards the corrosion through a simple screening effect, that is, causing only inactivation of a part of the surface with respect to the corrosive medium, without affecting the corrosion mechanism. Second, the significant effect of the inhibitor concentration on the corrosion potential may be explained in terms of the strong adsorption of S-alkyl isothioronium cations at the steel/solution interface. Third, at a given concentration, the inhibitor efficiency changes in the following order: VIII > VII > VI > V > IV > III > II > I. These findings are in accordance with results from OCP measurements.

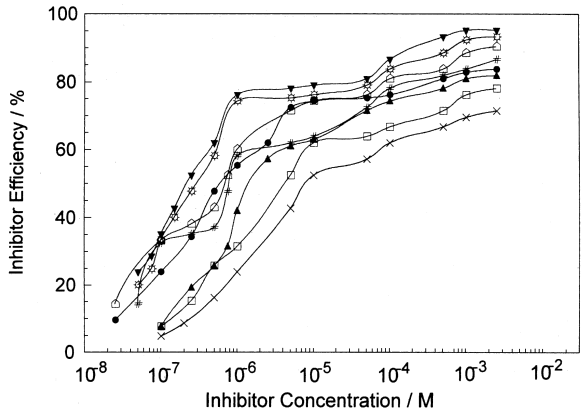

Fig. 4. Change in inhibitor efficiency with concentration of the S-alkyl isothioronium iodide. Key: (✳) I, (□) II, (▲) III, (●) IV, (#) V, (⌓) VI, (❋) VII, (▼) VIII.

3.2. *Effect of nature of halide counter ion of S-alkyl isothioronium halide on inhibition characteristics*

The change in OCP with time for steel coupons immersed in water from Western Desert crude oil with or without additions of S-*n*-octyl isothioronium bromide (IX) at 25 °C is similar to that observed in Figure 1. For low additive concentrations ($C \leqslant 1 \times 10^{-4}$ M), the OCP becomes more negative with increasing time. However, at higher concentration, ($C > 1 \times 10^{-4}$ M), the steady state was less negative. The dependence of the steady-

state potential (after about 300 min of immersion) on the concentration of inhibitor IX shows a single S shape, instead of the double S shape observed for iodide compounds, suggesting adsorption of bromide compound in a single layer. This behaviour suggests that the adsorption process in the presence of the bromide ion is competitive, rather than the cooperative adsorption that appears in the presence of iodide compound. The iodide counter ion is adsorbed on the steel surface forming a compact sublayer within the electrical double layer (EDL), leading to attraction of S-alkyl isothioronium cations ($SC(NH_2)_2^+$). In the case of the bromide compound, on the other hand, there is a competetive adsorption of the bromide ion and the S-alkyl isothioronium cation, forming one adsorbed layer within the EDL [14].

To compare the effect of the counter ion on the inhibitor efficiency, Figure 5 shows the change in inhibitor efficiency with the logarithm of concentration of inhibitors IX and VIII at 25 °C. Again, the inhibitor IX curve is characterized by one S-shape adsorption isotherm, indicative of monolayer adsorption. The inhibitor efficiency for VIII is much higher than for IX. This indicates that substitution of bromide ion by iodide ion greatly enhances the inhibitor efficiency. This conclusion agrees with the results of OCP measurements.

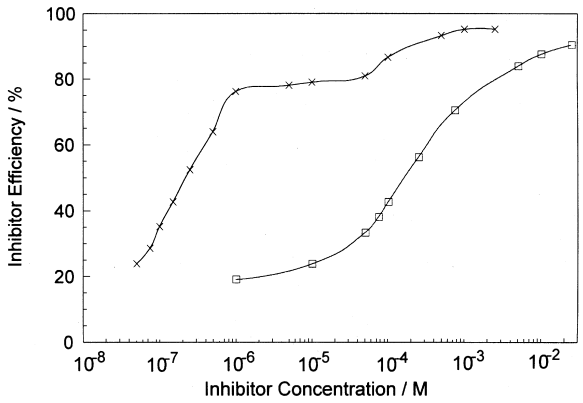

Fig. 5. Change in inhibitor efficiency with its concentration for S-*n*-octyl isothioronium iodide and S-*n*-octyl isothioronium bromide. Key: (×) S-*n*-octyl isothioronium iodide; (□) S-*n*-octyl isothioronium bromide.

3.3. *Kinetic–thermodynamic model and adsorption isotherm analyses*

In the present work we extended the application of a kinetic–thermodynamic model [16–18] to the inhibition of corrosion of steel in neutral medium. The data obtained from polarization measurements was fitted to the kinetic–thermodynamic model in terms of the number of active sites occupied by a single inhibitor molecule ($1/y$), the binding constant of the inhibitor with the metallic surface (K), and the change in free energy of adsorption (ΔG_{ads}.). These parameters are important for the understanding of the effect of structural changes in the inhibitor compound on the inhibition mechanism and efficiency. The experimental data were also fitted to Langmuir, Hill de Boer, Frumkin, Temkin, Parsons and Flory–Huggins adsorption isotherms. The data could only be well fitted to the Flory–Huggins adsorption isotherm and the kinetic–thermodynamic model, yielding a correlation coefficient higher than 0.98. The fitting to the Flory–Huggins isotherm [19] (Equation 4) for low concentrations of S-alkyl isothioronium iodides is shown in Figure 6.

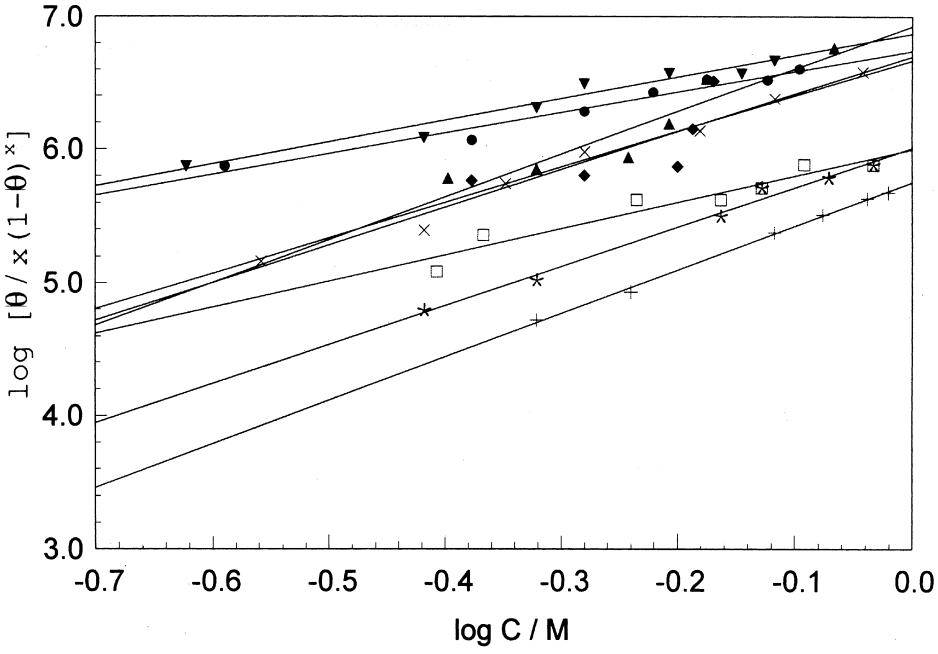

Fig. 6. Curve fitting of results for S-alkyl isothioronium iodides to the Flory–Huggins isotherm. Key: (+) I, (✳) II, (×) IV, (♦) V, (▲) VI, (●) VII, (▼) VIII.

$$\frac{\theta}{x(1-\theta)^x} = KC \tag{4}$$

where C is the inhibitor concentration in the bulk solution, x is the size parameter and is a measure of the number of adsorbed water molecules substituted by a given inhibitor molecule and θ is the surface coverage calculated from the following relationship:

$$\theta = \left(1 - \frac{i_{corr}}{(i_{corr})_o}\right) \tag{5}$$

Fitting of data for S-alkyl isothioronium iodide to the kinetic–thermodynamic model [16–18] (Equation 6) is presented in Figure 7.

$$\log\left(\frac{\theta}{1-\theta}\right) = \log K' + y \log C \tag{6}$$

$$K = K'^{(1/y)} \tag{7}$$

It is evident that the data are well fitted by straight lines. The slope of the lines is y, the number of inhibitor molecules occupying a single active site; the intercept is log K'. Table 4 summarizes the adsorption parameters as obtained from the kinetic–thermodynamic model and Flory–Huggins adsorption isotherm for S-alkyl isothioronium iodides. The value of K gradually increases from 1.34×10^5 to 45.71×10^5 for compounds I and VIII, respectively. This clearly indicates that the strength of electrical interactions between adsorbing molecules and the surface increases in the same order as mentioned previously, thus increasing the inhibitor efficiency. The results indicate reasonable agreement between the values of binding constant as obtained from the kinetic–thermodynamic model and the Flory–Huggins isotherm. The results also show that the $1/y$ values are greater than one, indicating that the S-alkyl isothioronium cation is mainly adsorbed at more than one active site of the metallic surface at 25 °C. The large negative values of the standard free energy of adsorption indicate that the reaction proceeds spontaneously and is accompanied by a highly efficient adsorption. The same calculations were made for compound IX and are reported in Table 4. The K value for inhibitor S-*n*-octyl isothioronium bromide, IX, is very small (0.04×10^5 compared to 45.71×10^5 for inhibitor S-*n*-octyl isothioronium iodide,

Table 4. Binding constant (K), number of active sites ($1/y$), and change of free energy obtained from the kinetic–thermodynamic model and the Flory–Huggins adsorption isotherm for S-alkyl isothioronium iodide

Inhibitor	Kinetic–thermodynamic model			Flory–Huggins isotherm		
	$1/y$	K /10^{-5}	ΔG^o_{ads} /kJmol^{-1}	x	K /10^{-5}	ΔG^o_{ads} /kJ mol^{-1}
I	1.52	1.34	−39.22	3.20	1.73	−39.80
II	1.60	2.50	−40.77	2.94	3.46	−41.56
III	1.32	4.96	−42.46	1.97	5.06	−42.51
IV	1.70	12.03	−44.66	2.80	17.69	−45.61
V	1.78	12.94	−44.84	2.67	17.53	−45.53
VI	1.87	17.04	−45.52	3.21	26.31	−46.60
VII	1.27	35.82	−47.37	1.50	35.45	−47.34
VIII	1.34	45.71	−47.97	1.63	45.49	−47.96
IX	3.32	0.04	−30.68	5.80	0.3	−35.51

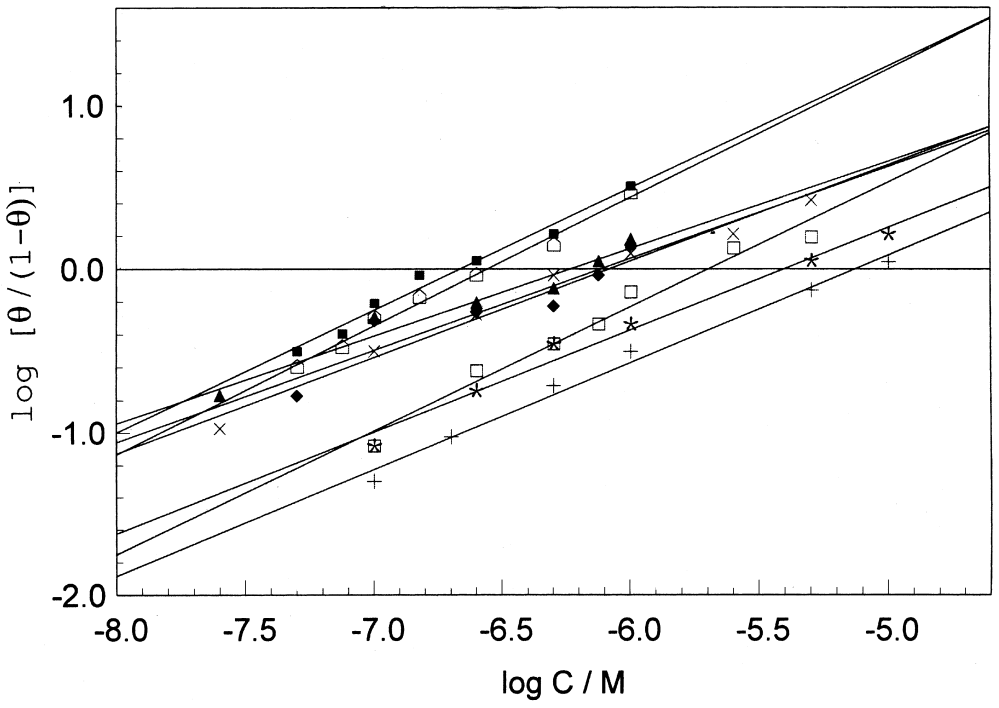

Fig. 7. Curve fitting of results from S-alkyl isothioronium iodides to the kinetic–thermodynamic model. Key: (+) I, (∗) II, (□) III, (×) IV, (♦) V, (▲) VI, (⌓) VII, (■) VIII.

VIII) indicating less adsorption of the bromide compound on steel surface. Moreover, the number of active sites occupied by one molecule of this compound is much higher (3.32), representing the enhanced number of centres of adsorption due to competitive adsorption.

References

1. B.D. Craig, *Mater. Perform.* **35** (1996) 61.
2. K.D. Efird and R.J. Jasinski, *Corrosion* **45** (1989) 165.
3. D.B. Lebsack and D. Hawn, *Mater. Perform.* **37** (1998) 24.
4. A.A. Gonik, *Zashchita Metallov* **32** (1996) 622.
5. M. Slack, *Mater. Perform.* **31** (1992) 49.
6. K.D. Efird, *Mater. Perform.* **30** (1991) 63.
7. B.G. Balashov and L.T. Shichalina, *Prot. Met.* **24** (1989) 758.
8. V.F. Voloshin, O.P. Golosova, L.A. Mazalevskaya, V.S. Bakumenko and A.K. Sheinkman, *Prot. Met.* **24** (1989) 685.
9. V.P. Redko, E.S. Ivanov, V.I. Frolov and Yu.A. Chirkov, *Prot. Met.* **25** (1990) 663.
10. A.A. EI-Hosary, R.M. Saleh and A.O. Abdel Fattah, Proceedings of the 8th European Symposium on 'Corrosion Inhibition,' Ann. Univ. Ferrara, No. 10 (1995), 1269.
11. S.A. Nesterenko, V.I. Sorokin, O.V. Naumenko and E. Yu. Melanich, *Prot. Met.* **24** (1989) 413.
12. O.V. Vasilenko, P.A. Zhdan, Yu.N. Shekhter, G.D. Chukin, N.I. Korokh, T.I. Boganova and I.I. Skarzov, *Prot. Met.* **23** (1988) 756.
13. A.J. McMahon, *Colloids Surf.* **59** (1991) 187.
14. B.A. Abd El-Nabey, E. Khamis, M.Sh. Ramadan and A. El-Gindy, *Corrosion* **52** (1996) 671.
15. H. Fischer, *Werkst. Korros.* **96** (1973) 575.
16. A.A. El-Awady, B.A. Abd-El-Nabey, S.G. Aziz, M.A. Khalifa and H.A. Ghamedy, *Int. J. Chem.* **1** (1990) 169.
17. A.A. El-Awady, B.A. Abd-El-Nabey, and S.G. Aziz, *J. Electrochem. Soc.* **139** (1992) 2149.
18. A.A. El-Awady, B.A. Abd-El-Nabey and S.G. Aziz, *J. Chem. Soc.* **89** (1993) 795.
19. H. Dhar, B. Conway and K. Joshi, *Electrochim. Acta* **18** (1973) 789.